Finite element method for 3D optical modeling of liquid crystal on silicon spatial light modulator

Chen, Po Ju; Engel, Philip; Mazur, Adam; Abélard, Clément; Urbach, H. Paul

Important note
To cite this publication, please use the final published version (if applicable).
Please check the document version above.

PROCEEDINGS OF SPIE

Finite element method for 3D optical modeling of liquid crystal on silicon spatial light modulator

Chen, Po-Ju, Engel, Philip, Mazur, Adam, Abélard, Clément, Urbach, H. Paul

Finite element method for 3D optical modeling of liquid crystal on silicon spatial light modulator

Po-Ju Chen[a,b*], Philip Engel[b], Adam Mazur[b], Clément Abélard[b], and H. Paul Urbach[a]

[a]Optics Research Group, Delft University of Technology, Lorentzweg 1, 2628 CJ Delft, The Netherlands
[b]HOLOEYE Photonics AG, Volmerstr. 1, 12489 Berlin, Germany

ABSTRACT

Accurate optical modeling for design and optimization of liquid crystal on silicon spatial light modulators (LCoS SLMs) is important for phase-related applications. Traditional matrix method cannot accurately predict the optical performance when the LC distribution is complex, therefore the rigorous finite element method (FEM) is preferred. However, the optical modeling of LCoS is a multidimensional problem, which is difficult to simulate with FEM. Here, we present the development of an improved FEM by combining the scattering matrix method with the domain decomposition method to reduce the computational burden for optical simulation of LCoS. Furthermore, a 2D simulation example with phase grating displayed on LCoS is presented and compared with experiment.

Keywords: Liquid Crystal on Silicon, spatial light modulator, LCoS, beam steering, diffractive optics, finite element method

1. INTRODUCTION

Liquid crystal on silicon (LCoS) spatial light modulator (SLM) can be applied to many optical systems to control the phase distribution spatially. For example, for the application of beam steering in telecommunication, LCoS SLM are uesd to displayed different phase pattern to create different phase grating to change the propagation direction of incident beam.[1,2] Also, LCoS SLM can be used to create structured light for complex and customized light field.[3,4] For these and other applications, it is important to design and optimize the optical performance of the LCoS SLM for maximum diffraction efficiency. However, this is not an easy task due to the fact that the LCoS SLM is a multiscale structure.[5] The typical structure of LCoS SLM is shown as in Fig.1. The thickness of the glass substrate is in the range of a few millimeters to hundreds of micrometers. To enhance the optical transmittance, sometimes the anti-reflection coating layer is deposited on top. Below the glass substrate, an index matched indium tin oxide (IMITO) layer is presented with thickness in the range of tens of nanometers followed by alignment layer with tens of nanometers. The next layer is arguably the most important in our simulation because it consists of the liquid crystal layer. It has thickness of several micrometers.The optimization of the thickness of the LC layer is important in the design of SLM for different wavelengths. Finally, after the bottom alignment layer comes the backplane. The backplane consists the silicon oxide layer with thickness of several tens of nanometers on top of an aluminum grating with thickness hundreds of nanometers.

For design and optimization of specific applications, accurate optical simulation methods is important. Besides the problem mentioned at the beginning, another difficulty appears when trying to simulate phase pattern with longer period. Since not only the actively changed LC layer but also the the absorptive pixelated backplane with fixed designed parameters have to be simulated properly, this essentially consume more memory and time for the optical simulation to achieve right accuracy.

In this paper, we describe a rigorous optical simulation method which combines two different rigorous optical simulation methods, namely finite element method[6] and rigorous coupled wave analysis method(RCWA)[7] for optical simulation of LCoS SLM. In the next section we explain the theoretical idea and a simulation result of the 2D fictitious binary phase grating displayed on LCoS SLM is given. Finally, we compare the simulation with experiment results of a blazed grating.

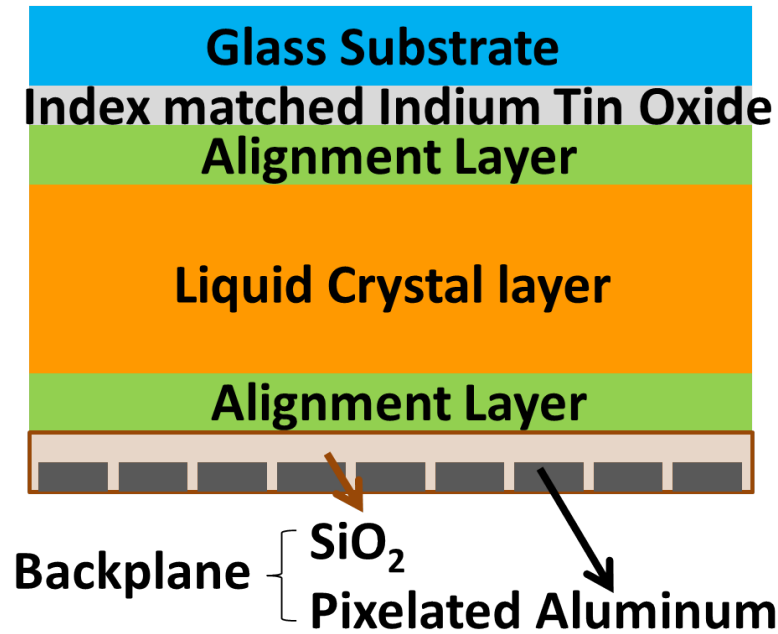Email: po-ju.chen@holoeye.com / p.chen-4@tudelft.nl

Figure 1. Simulation structure of a typical LCoS SLM.

2. HYBRID METHOD: COMBINATION OF DIFFERENT OPTICAL SIMULATION APPROACHES

In this section, we describe the domain decomposition method with combination of a non-iterative scattering matrix method, which is used on solving Maxwell's equation with finite element methods.[8] The domain decomposition method divides the whole computation domain Ω to smaller subdomain $\Omega_i, i = 1, 2, ..., l$. Each domain solves for a smaller boundary value problem. Considering the fact that the total near field along the boundaries of each subdomain can be transformed into the combination of Fourier plane waves under periodic boundary condition. We can assume each incident Fourier plane wave with unit amplitude, and calculate the corresponding scattering field and rearrange the Fourier coefficients of the scattering field of each Fourier modes into the format of the scattering matrix for each domain. With the continuous field boundary condition between subdomains, we can arrange the scattering matrix into a stack matrix together with an unknown weighted vector that describe the coupling condition between subdomains. By applying the illumination condition from the top or bottom exterior domain, we can solve the unknown weighted vector and retrieve the optical response that we are looking for.

Nevertheless, for the thick multilayers with homogeneous optical properties, i.e. glass substrate and index matched indium tin oxide layer, it is not efficient to use the finite element method for simulation. As a result, we extend the method with combination of rigorous coupled wave analysis method[9, 10] to calculate the scattering matrix of the thick multilayers on top domain. The calculation procedure is similar to that of FEM, where we calculate the Fourier coefficients of the scattering field with respect to each incident Fourier plane waves.

2.1 Single Domain Case

For single domain Ω_i, we first assume transparent boundary conditions for boundary surfaces which are perpendicular to the $z-$axis and periodic boundary conditions for the boundary surfaces which are perpendicular to the $x-$ or $y-$axis.Let the refractive index in the exterior domain on top (Ω_i^{top}) and bottom (Ω_i^{btm}) equal to n_i^{top} and n_i^{btm} respectively, as shown in Fig.2. This means the refractive index on top and bottom satisfied $n_i^{top/btm}(x, y, z) = n_i^{top/btm}(x + \Lambda_x, y + \Lambda_y, z)$. Thus, the incident wave vector $\mathbf{k}_{m,top/btm}^{i,+/-}$ which indicate that the

wave either propagating upward(+) or downward(-) from top exterior domain or bottom exterior domain can be defined as,

$$\mathbf{k}_{m,top/btm}^{i,+/-} = (k_{m,x}, k_{m,y}, \pm\sqrt{(k_{top/btm}^i)^2 - k_{m,x}^2 - k_{m,y}^2}) \tag{1}$$

,where $k_{top/btm}^i = \frac{2\pi n_{top/btm}^i}{\lambda_0}$, λ_0 is the wavelength in vacuum, and $k_{m,x} = k_x + \frac{2\pi m_1}{\Lambda_x}$, $k_{m,y} = k_y + \frac{2\pi m_2}{\Lambda_y}$, m = 1,2,...,M. Here m is the index that indicate the pair combination of diffraction orders in x and y direction, i.e. m = 1 means $(m_1, m_2) = (0,0)$, m =2 means $(m_1, m_2) = (1,0)$, etc. M is the maximum diffraction order where incident light field is a propagated rather than evanescent field.

Then, we define the unknown incident electric field $\mathbf{E}_{in}^-(\mathbf{r})$ propagate downward from top to bottom and also the unknown incident electric propagate from bottom to top $\mathbf{E}_{in}^+(\mathbf{r})$. The Fourier transform of the incident electric field can be expressed as following,

$$\mathbf{E}_{in}^{i,-}(\mathbf{r}) = \sum_{m=1}^{M} w_m^{i,top,-}\widehat{\mathbf{E}}_m^{i,top,-} e^{i\mathbf{k}_{m,top}^{i,-}\cdot\mathbf{r}}, \tag{2}$$

$$\mathbf{E}_{in}^{i,+}(\mathbf{r}) = \sum_{m=1}^{M} w_m^{i,btm,+}\widehat{\mathbf{E}}_m^{i,btm,+} e^{i\mathbf{k}_{m,btm}^{i,+}\cdot\mathbf{r}}, \tag{3}$$

, where $\widehat{\mathbf{E}}_m^{i,top/btm}$ is the field component, $w_m^{i,top/btm,+/-}$ is the weight of basis vector.

We further arrange the terms $\widehat{\mathbf{E}}_m^{i,top/btm,+/-}$ as vector components of $\widehat{\mathbf{E}}_i^{top,-}$ and $\widehat{\mathbf{E}}_i^{btm,+}$ for the convenient of representation and calculation. So the Fourier coefficients of $\mathbf{E}_{in}^{i,+/-}$ can be expressed as the product of weight matrix $\underline{\underline{W_i}}$ and k-space basis vector $\widehat{\mathbf{E}}_i$ as following,

$$\widehat{\mathbf{E}}_{in}^{i,-} = \underline{\underline{W_i}}^{top,-}\widehat{\mathbf{E}}_i^{top,-}, \tag{4}$$

$$\widehat{\mathbf{E}}_{in}^{i,+} = \underline{\underline{W_i}}^{btm,+}\widehat{\mathbf{E}}_i^{btm,+}, \tag{5}$$

where $\underline{\underline{W_i}}^{top/btm}$ is the diagonal matrix with diagonal entries equal to $w_n^{i,top/btm,+/-}$.

The corresponding Fourier coefficients of the scattering field induced by E_{in}^- is equal to

$$\widehat{\mathbf{E}}_{sc}^{i,+} = \underline{\underline{W_i}}^{top,+}\underline{\underline{R_i}}^{1,1}\widehat{\mathbf{E}}_i^{top,+}, \tag{6}$$

$$\widehat{\mathbf{E}}_{sc}^{i,-} = \underline{\underline{W_i}}^{btm,-}\underline{\underline{T_i}}^{2,1}\widehat{\mathbf{E}}_i^{top,-}, \tag{7}$$

, where $\underline{\underline{R_i}}^{1,1}$ is the scattering matrix where each row contains the reflection coefficients of each incident Fourier plane wave mode and upper notation means the field coming from top exterior domain (1) and reflected back also in the same domain (1). $\underline{\underline{T_i}}^{2,1}$ is the scattering matrix where each row contains the transmission coefficients of each incident Fourier plane wave mode and the upper notation means the field coming from the top exterior domain (1) and transmitted to the bottom exterior domain (2). This is similar for the scattering field when the incident field $\mathbf{E}_{in}^+$ coming from bottom exterior domain,

$$\widehat{\mathbf{E}}_{sc}^{i,+} = \underline{\underline{W_i}}^{top,+}\underline{\underline{T_i}}^{1,2}\widehat{\mathbf{E}}_i^{btm,+}, \tag{8}$$

$$\widehat{\mathbf{E}}_{sc}^{i,-} = \underline{\underline{W_i}}^{btm,-}\underline{\underline{R_i}}^{2,2}\widehat{\mathbf{E}}_i^{btm,-}. \tag{9}$$
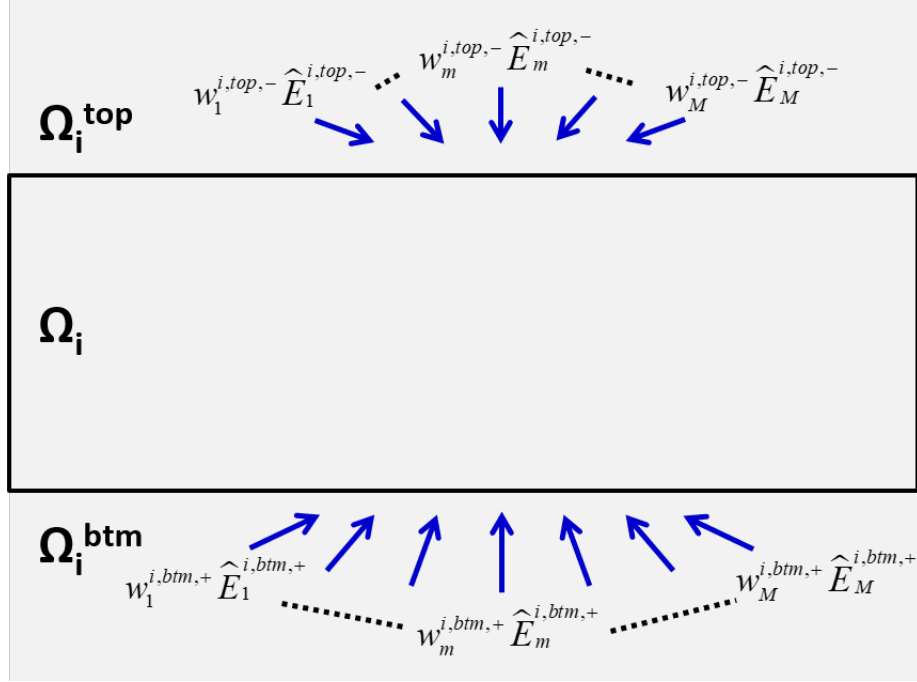
Figure 2. FEM simulation of the scattering matrix for single domain

2.2 Multiple Subdomains Case

To combine the multiple subdomains, the electromagnetic field have to satisfied the interface coupling condition between subdomains. The field on the boundary Γ_i have to be continuous, which means the total field $\mathbf{E}_{total} = \mathbf{E}_{in} + \mathbf{E}_{sc}$ from Ω_i^{btm} and Ω_{i+1}^{top} should be the same for i = 1,2,..,P. Take our simulation structure in Fig.3 as an example, the total field from Ω_1^{btm} should be equal to the field from Ω_2^{top}.

The total field at Ω_1^{btm} are

$$
\begin{aligned}
\widehat{\mathbf{E}}_{in}^1 &= \underline{\underline{W_1}}^{btm,+}\widehat{\mathbf{E}}_1^{btm,+}, \\
\widehat{\mathbf{E}}_{sc}^1 &= \underline{\underline{W_1}}^{btm,-}\underline{\underline{R_1}}^{2,2}\widehat{\mathbf{E}}_1^{btm,-} + \underline{\underline{W_1}}^{btm,-}\underline{\underline{T_1}}^{2,1}\widehat{\mathbf{E}}_1^{top,-}.
\end{aligned}
\tag{10}
$$

And for the total field at Ω_2^{top} are

$$
\begin{aligned}
\widehat{\mathbf{E}}_{in}^2 &= \underline{\underline{W_2}}^{top,-}\widehat{\mathbf{E}}_2^{top,-}, \\
\widehat{\mathbf{E}}_{sc}^2 &= \underline{\underline{W_2}}^{top,+}\underline{\underline{R_2}}^{1,1}\widehat{\mathbf{E}}_2^{top,+} + \underline{\underline{W_2}}^{top,+}\underline{\underline{T_2}}^{1,2}\widehat{\mathbf{E}}_2^{btm,+}.
\end{aligned}
\tag{11}
$$

So the total field that should be equivalent at the boundary Γ_1 are,

$$
\begin{aligned}
\underline{\underline{W_1}}^{btm,+}\widehat{\mathbf{E}}_1^{btm,+} + \underline{\underline{W_1}}^{btm,-}\underline{\underline{R_1}}^{2,2}\widehat{\mathbf{E}}_1^{btm,-} + \underline{\underline{W_1}}^{btm,-}\underline{\underline{T_1}}^{2,1}\widehat{\mathbf{E}}_1^{top,-} = \\
\underline{\underline{W_2}}^{top,-}\widehat{\mathbf{E}}_2^{top,-} + \underline{\underline{W_2}}^{top,+}\underline{\underline{R_2}}^{1,1}\widehat{\mathbf{E}}_2^{top,+} + \underline{\underline{W_2}}^{top,+}\underline{\underline{T_2}}^{1,2}\widehat{\mathbf{E}}_2^{btm,+}.
\end{aligned}
\tag{12}
$$

Since the medium at Ω_1^{btm} and Ω_2^{top} is the same, the field that propagate in same direction should match to each other along the boundary Γ_1. So the following equations can be derived,

$$
\begin{aligned}
\underline{\underline{W}}^+ &: \quad \widehat{\mathbf{E}}_1^{btm,+} = \underline{\underline{R_2}}^{1,1}\widehat{\mathbf{E}}_2^{top,+} + \underline{\underline{T_2}}^{1,2}\widehat{\mathbf{E}}^{btm,+}, \\
\underline{\underline{W}}^- &: \quad \widehat{\mathbf{E}}_2^{top,-} = \underline{\underline{R_1}}^{2,2}\widehat{\mathbf{E}}^{btm,-} + \underline{\underline{T_1}}^{2,1}\widehat{\mathbf{E}}^{top,-},
\end{aligned}
\tag{13}
$$

By combining all the interface coupling conditions, we retrieve a stack matrix $\underline{\underline{S}}$ and the vector $\widehat{\mathbf{E}}$ with the vector component of the unknown incident Fourier coefficients vector $\widehat{\mathbf{E}}_i^{top/btm}$ at different subdomains,

$$\underline{\underline{S}}\widehat{\mathbf{E}} = \begin{bmatrix} \underline{\underline{I}} & & & & & \\ -\underline{\underline{T_1}}^{2,1} & -\underline{\underline{R_1}}^{2,2} & \underline{\underline{I}} & & & \\ & \underline{\underline{I}} & -\underline{\underline{R_2}}^{1,1} & -\underline{\underline{T_2}}^{1,2} & & \\ & -\underline{\underline{T_2}}^{2,1} & -\underline{\underline{R_2}}^{2,2} & \underline{\underline{I}} & & \\ & & & \underline{\underline{I}} & -\underline{\underline{R_3}}^{1,1} & -\underline{\underline{T_3}}^{1,2} \\ & & & & & \underline{\underline{I}} \end{bmatrix} \begin{bmatrix} \widehat{\mathbf{E}}_1^{top,-} \\ \widehat{\mathbf{E}}_1^{btm,+} \\ \widehat{\mathbf{E}}_2^{top,-} \\ \widehat{\mathbf{E}}_2^{btm,+} \\ \widehat{\mathbf{E}}_3^{top,-} \\ \widehat{\mathbf{E}}_3^{btm,+} \end{bmatrix}, \tag{14}$$

For the information of coming illuminated light source either from the top exterior domain (Ω_1^{top}) or bottom exterior domain (Ω_3^{btm}) is in vector s_{in}. The relation of s_{in} between stack matrix and weighted vector are shown as

$$\underline{\underline{S}}\widehat{\mathbf{E}} = \mathbf{s}_{in} \tag{15}$$

The unknown $\widehat{\mathbf{E}}$ can be computed by

$$\widehat{\mathbf{E}} = \underline{\underline{S}}^{-1} s_{in} \tag{16}$$

Figure 3.   Applying domain decomposition method to the LCoS structure, each subdomain is isolated with fictitious exterior domain at bottom or top, where the thickness of the exterior domains approach zero.

3. SIMULATION AND EXPERIMENT RESULTS OF PHASE GRATING

3.1 Simulation of Binary Grating

To validate the proposed method, we choose a fictitious 2D binary grating with 2 pixels per period as our simulation target. The periodicity in (x,y) direction of the simulation structure is set to (7.48, 0) for 2D

with unit equal to μm. The wavelength is set to 633 nm with normal incidence. We first separate the whole simulation domain into three parts as mentioned above. The scattering matrix of the top domain (Γ_1), consist only a fictitious glass substrate with a thickness of 600 nm, was pre-calculated by the RCWA methods. As for the middle part(Γ_2), we begin with performing the simulation of the LC director with different applied voltage (V_{on}) for one pixel with LCDmaster (Shintech) to find the π phase shift in 2D simulation. With the finding of the applied voltage that leads to π phase shift, we further set the applied voltage of pixels of the binary grating to 0 and V_{on} respectively to obtain the spatial rotation distribution of the LC director profile. The direction of the grating period is perpendicular to the LC rubbing direction, i.e. rubbing direction is y-axis. Then, the output of the twist and tilt angle of LC directors are transformed to permittivity tensors in space coordinate as the input for the FEM simulation software, JCMsuite (JCMwave). Finally, the bottom part (Γ_3) is also simulated with the FEM to obtain the scattering matrix.

The simulation results are shown in Fig. 4. The result of proposed hybrid method are shown with the green histogram (FEM_RCWA_SC). The comparison which uses the FEM to calculate the scattering matrix of the top domain is shown as the blue histogram (FEM_SC). Due to the assumption of the thin glass substrate, we can simulate the whole simulation domain together (Γ_1 to Γ_3) with only the FEM method, which is shown as the red histogram (FEM). The simulation results of the diffraction efficiency among different methods are agreed well with each other. And the total diffraction efficiency of proposed hybrid method (FEM_RCWA_SC), FEM combined with scattering method(FEM_SC) and FEM-only (FEM) are 84.92%, 84.93% and 84.67%, respectively, which is pretty similar to each other with a difference less than 0.5%. The comparison of the simulation results has shown our concept works.
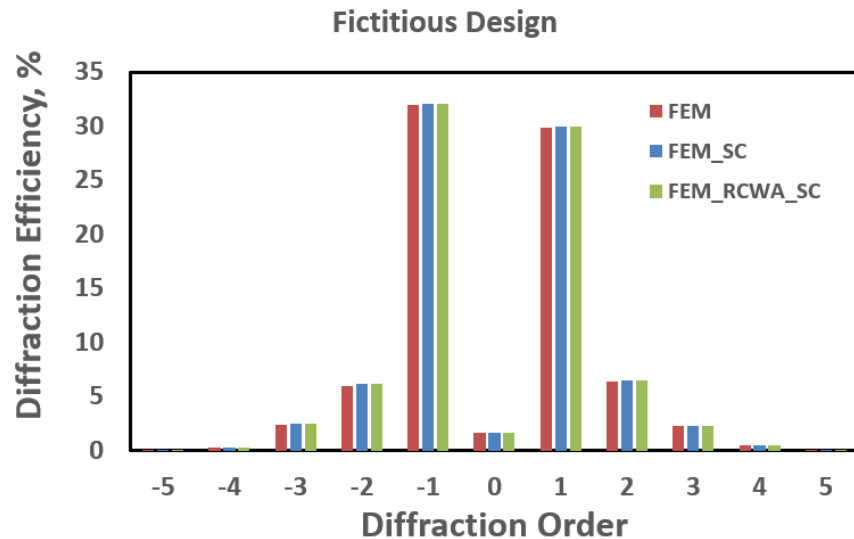

Figure 4. The simulation results of 2D binary phase grating with 2 pixels per period. The green histogram has shown the result of the proposed hybrid method which combines FEM, RCWA and scattering matrix method (FEM_RCWA_SC). The blue histogram has shown the result of the combination of FEM and scattering matrix methods (FEM_SC). The red histogram has shown the result of using only FEM on whole simulation domain (FEM).

3.2 Comparison Between Simulation and Experiment Results

Here we performed the experiment with the set-up mentioned in previous article[11] to measure the grey level of the LCoS. The incident wavelength is equal to 1550 nm. We measured the diffraction efficiency of the blazed grating with 6 pixels per period and the pixel pitch is equal to 8 μm, which means the total period of the grating is 48 μm. By using the measured and linearized grey level, we simulated the corresponding 2D LC director distribution of the blazed grating. With the 2D LC director profile, we performed the 2D optical simulation with period equal to (x,y) = (48, 0). The experiment and simulation results are as shown in Fig. 5. The

experiment result are shown with red histogram, which is normalized with the measured incident laser power. Both the simulation results of FEM combining transfer matrix method (yellow histogram)[12] and the proposed hybrid method (green histogram) agree with each other and correctly predict the optical performance of the blazed grating.
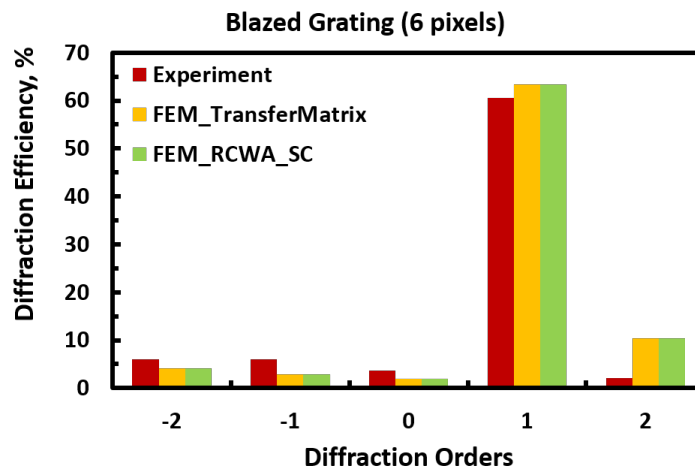

Figure 5. The experiment and simulation results of the blazed grating with 6 pixels per period for incident wavelength of 1550nm.

4. CONCLUSION

In this article, we proposed a 3D hybrid rigorous optical simulation method that combines FEM with RCWA through domain decomposition method and the scattering matrix method. The 2D simulation results of the fictitious binary grating with 2 pixels per period have shown a good agreement among different methods, the proposed hybrid rigorous simulation method, FEM that combined with scattering matrix method and FEM-only, which prove our concept work. The simulation and experiment results of the blazed grating with 6 pixels per period are agreed with each other. Furthermore, the 2D simulation result of the proposed hybrid method agrees with the traditional iterative simulation method, which the FEM combines with the transfer matrix method. So with the proposed non-iterative hybrid method, we only need to calculate the optical response of the top and bottom part of the LCoS SLM once and focus on the optical simulation of the LC layer under the same periodicity, which facilitate the rigorous optical simulation of the LCoS SLM.

ACKNOWLEDGMENTS

REFERENCES

[1] Apter, B., Efron, U., and Bahat-Treidel, E., "On the fringing-field effect in liquid-crystal beam-steering devices," *Applied optics* **43**(1), 11–19 (2004).

[2] Fontaine, N. K., Chen, H., Ercan, B., Ryf, R., Labroille, G., Barre, N., Jian, P., Morizur, J. F., and Neilson, D. T., "Wavelength selective switch with optimal steering element utilization," in [*2016 Optical Fiber Communications Conference and Exhibition (OFC)*], 1–3, IEEE (2016).

[3] Rubinsztein-Dunlop, H., Forbes, A., Berry, M., Dennis, M., Andrews, D. L., Mansuripur, M., Denz, C., Alpmann, C., Banzer, P., Bauer, T., et al., "Roadmap on structured light," *Journal of Optics* **19**(1), 013001 (2016).

[4] Forbes, A., Dudley, A., and McLaren, M., "Creation and detection of optical modes with spatial light modulators," *Advances in Optics and Photonics* **8**, 200–227 (2016).

[5] Lazarev, G., Chen, P.-J., Strauss, J., Fontaine, N., and Forbes, A., "Beyond the display: phase-only liquid crystal on silicon devices and their applications in photonics [invited]," *Opt. Express* **27**, 16206–16249 (May 2019).

[6] Monk, P., "Finite element methods for maxwell's equations," (Apr 2003).

[7] Moharam, M. G., Grann, E. B., Pommet, D. A., and Gaylord, T. K., "Formulation for stable and efficient implementation of the rigorous coupled-wave analysis of binary gratings," *J. Opt. Soc. Am. A* **12**, 1068–1076 (May 1995).

[8] Hammerschmidt, M., *Optical simulation of complex nanostructured solar cells with a reduced basis method*, PhD thesis (2016).

[9] Lalanne, P. and Jurek, M. P., "Computation of the near-field pattern with the coupled-wave method for transverse magnetic polarization," *Journal of Modern Optics* **45**(7), 1357–1374 (1998).

[10] Hugonin, J. P. and Lalanne, P. *Reticolo software for grating analysis* (2005).

[11] Chen, P.-J., Engel, P., Lazarev, G., Mazur, A., and Urbach, P., "Design, implementation, and study of the high-resolution high-efficiency liquid crystal on silicon spatial light modulator for the telecommunication application in the short-wave infrared spectral band," *Proc.SPIE* **10941**, 10941 – 10941 – 13 (2019).

[12] Schädle, A., Zschiedrich, L., Burger, S., Klose, R., and Schmidt, F., "Domain decomposition method for maxwell's equations: Scattering off periodic structures," *Journal of Computational Physics* **226**(1), 477 – 493 (2007).